SCIENTIFIC REPORTS

OPEN

Influence of oxygen on generation of reactive chemicals from nitrogen plasma jet

Received: 11 January 2018
Accepted: 4 June 2018
Published online: 18 June 2018

Han Sup Uhm[1], Se Hoon Ki[2], Ku Youn Baik[2] & Eun Ha Choi[2]

A nonthermal plasma jet is operated at atmospheric pressure inside a vacuum chamber filled with nitrogen gas. Various chemical compounds are fabricated from nitrogen and water molecules in plasma jet with varying oxygen content. Detailed theoretical investigation of these chemical compounds is carried out in terms of different oxygen ratio ξ. Experimental measurements are also carried out for comparison with theoretical results. Hydroxyl molecules are mostly generated at surface of water, and some of them can penetrate into water. The density of hydroxyl molecules has its maximum without oxygen, and decreases to zero as ξ increases to 0.25. The density of the ammonia of NH_3 also deceases as ξ increases to 0.25. On the other hand, theory and experiment show that the density of the NO_3 increases drastically as ξ increases to 0.25. The hydrogen peroxide density in plasma activated water deceases, reaches its minimum value at $\xi = 0.05$, and then increases again, as ξ increases from a small value to a large value. The *pH* value of the plasma activated water, which is slightly changed to alkali without oxygen, decreases as ξ increases.

Nonthermal plasma was proposed as a novel therapy for some incurable diseases[1–6]. Nonthermal plasma generates various kinds of reactive chemicals including reactive oxygen species (ROS) and reactive nitrogen species (RNS) in the liquid, and the consequent increase of intracellular ROS and RNS have been reported as main cause for various biological events. In recent studies, plasma activated water/media showed similar anticancer effects as direct nonthermal plasma treatment[7,8]. These reports support that those diseases may be cured by long lived ROS/RNS. H_2O_2 and $ONOO^-$ have been suggested as main players in plasma treated liquids[8–10]. However, still it is unclear why any artificial combination of H_2O_2 and NO_2^- cannot make full biological effects as plasma does. Therefore, the effects of different compositions of reactive species in the plasma need to be investigated.

Nitrogen plasma is known to produce OH radicals easily according to the water bombardment of excited nitrogen molecules in a metastable state[11]. Though OH radicals from the liquid surface are hard to directly affect biological systems, the OH radicals are important source to generate H_2O_2 or $ONOO^-$. In addition, oxygen addition to the nitrogen gas causes dramatic changes in the chemistry of plasma treated water, resulting in differential biological responses[12–15]. Therefore, this article investigates influence of oxygen on generation of reactive species in nitrogen plasma.

In this study, detailed theoretical investigation of these chemical compounds is carried out in terms of different oxygen content (1~25%). The steady-state density of the H, OH, HO_2, H_2O_2, NH, NH_2, NH_3, NO, HNO_2, and HNO_3 are calculated using major forty two chemical reactions (Table 1). Experimental measurements are also carried out in comparison with theoretical results. OH, NH_4^+, H_2O_2, NO_3^-, and pH are measured in deionized water treated with nonthermal plasma. Though our analysis does not show detail kinetics in a pico second range or detail spatial distributions in a micro meter range as other computational simulation studies, our steady-state solutions are well matched with experimental measurements. This is the first report showing the changes in the chemical species in water according to the O_2 mole fraction in N_2 plasma in both theoretical and experimental approaches. Densities of H, OH, H_2O_2, NH, NH_2, and NH_3 drastically reduced in the low level of O_2 mole fraction, but densities of O and HNO_3 increased according to O_2 mole fraction. Their relations with the pH will be discussed.

We calculated the changes in the chemical reactive species in water according to the O_2 mole fraction in accordance with experiments.

[1]New Industry Convergence Technology R&D Center, Ajou University, Suwon, 16499, Republic of Korea. [2]Electrical and Biological Physics, Kwangwoon University, Seoul, 01897, Republic of Korea. Correspondence and requests for materials should be addressed to H.S.U. (email: hsuhm1970@gmail.com) or K.Y.B. (email: kybaik@kw.ac.kr)

Eq. Num.	Reaction	Rate coefficient	Ref.
1	$N_2 + e \rightarrow N_2(A_3\sum_u^+)$	$\alpha_{N2*} = 6.4 \times 10^{-12}\,cm^3/s$	
2	$N_2 + e \rightarrow 2N$	$k_N = 1 \times 10^{-12}\,cm^3/s$	
3	$O_2 + e \rightarrow 2O$	$k_O = 1.5 \times 10^{-11}\,cm^3/s$	
4	$N_2(A_3\sum_u^+) + H_2O \rightarrow OH + H + N_2$	$\alpha_{OH} = 5 \times 10^{-14}\,cm^3/s$	[18]
5	$N_2(A_3\sum_u^+) + N_2 \rightarrow N_2 + N_2$	$\alpha_{N2} = 3 \times 10^{-18}\,cm^3/molecule/s$	[18]
6	$N_2(A_3\sum_u^+) + O_2 \rightarrow products$	$\alpha_{O2} = 2.5 \times 10^{-12}\,cm^3/molecule/s$	[18]
7	$OH + H + M \rightarrow H_2O + M$	$\alpha_{H2O} = 1.14 \times 10^{-10}\,cm^3/mole/s$	[19]
8	$H + O_2 + M \rightarrow HO_2 + M$	$\alpha_{O2H} = 4.6 \times 10^{-13}\,cm^3/s$	[19]
9	$OH + OH + M \rightarrow H_2O_2 + M$	$\alpha_{H2O2} = 1.78 \times 10^{-11}\,cm^3/mole/s$	[21]
10	$OH + HO_2 \rightarrow H_2O + O_2$	$\alpha_{OH2} = 1.1 \times 10^{-10}\,cm^3/s$	[21]
11	$OH + H_2O_2 \rightarrow HO_2 + H_2O$	$\alpha_{HO2} = 1.7 \times 10^{-12}\,cm^3/s$	[21]
12	$HO_2 + HO_2 \rightarrow H_2O_2 + O_2$	$\alpha_{H2O2} = 1.24 \times 10^{-12}\,cm^3/molecules/s$	[22]
13	$H_2O_2 + O \rightarrow HO_2 + OH$	$\alpha_{HO2} = 1.7 \times 10^{-15}\,cm^3/molecules/s$	[21]
14	$HO_2 + H_2O_2 \rightarrow OH + H_2O + O_2$	$1 \times 10^{-13}\,cm^3/molecules/s$	[23]
15	$H_2O_2 + H \rightarrow OH + H_2O$	$4.2 \times 10^{-14}\,cm^3/molecules/s$	[19]
16	$H + N \rightarrow NH$	$\alpha_{NH} = 1.3 \times 10^{-12}\,cm^3/s$	[26]
17	$NH + OH \rightarrow HNO + H$	$\alpha_{HNO} = 3.32 \times 10^{-11}\,cm^3/s$	[27]
18	$NH + O \rightarrow OH + N$	$\alpha_{OH} = 1.16 \times 10^{-11}\,cm^3/molecules/s$	[28]
19	$NH + O_2 \rightarrow Products$	$\alpha_{Pro} = 9.98 \times 10^{-15}\,cm^3/molecules/s$	[26]
20	$NH + NH \rightarrow NH_2 + N$	$\alpha_{NH2} = 4.3 \times 10^{-13}\,cm^3/s$	[29]
21	$NH_2 + OH \rightarrow NH_2OH$	$\alpha_{NH2OH} = 9.31 \times 10^{-11}\,cm^3/s$	[30]
22	$NH_2 + O \rightarrow H + HNO$	$\alpha_H = 7.47 \times 10^{-11}\,cm^3/molecules/s$	
23	$O_2 + NH_2 \rightarrow H_2NOO$	$\alpha_{H2NOO} = 1.54 \times 10^{-15}\,cm^3/molecules/s$	
24	$H + NH_2 \rightarrow NH_3$	$\alpha_{NH3} = 7.7 \times 10^{-11}\,cm^3/molecules/s$	[31]
25	$HNO_3 + NH_2 \rightarrow NH_3 + NO_3$	$\alpha_{H3N} = 3.64 \times 10^{-13}\,cm^3/molecules/s$	[32]
26	$NH_3 + O \rightarrow OH + NH_2$	$\alpha_{OHN2} = 4.69 \times 10^{-17}\,cm^3/molecules/s$	[27]
27	$OH + NH_3 \rightarrow H_2O + NH_2$	$\alpha_{H2O} = 1.6 \times 10^{-13}\,cm^3/molecules/s$	[21]
28	$NH_3 + NO_3 \rightarrow HNO_3 + NH_2$	$\alpha_{HNO3} = 6 \times 10^{-16}\,cm^3/molecules/s$	[33]
29	$OH + N \rightarrow NO + H$	$\alpha_{ON} = 4.7 \times 10^{-11}\,cm^3/molecules/s$	[19]
30	$N + O \rightarrow NO$	$\alpha_{NO} = 2.39 \times 10^{-13}\,cm^3/mole/s$	[25]
31	$N + O_2 \rightarrow NO + O$	$\alpha_{NO} = 9.22 \times 10^{-17}\,cm^3/mole/s$	[22]
32	$NO + H \rightarrow HNO$	$\alpha_{HNO} = 1.56 \times 10^{-12}\,cm^3/molecules/s$	[34]
33	$NO + OH \rightarrow HNO_2$	$\alpha_{HNO2} = 1.78 \times 10^{-11}\,cm^3/s$	[22]
34	$HNO_2 + OH \rightarrow H_2O + NO_2$	$\alpha_{NO2} = 5.95 \times 10^{-12}\,cm^3/s$	[21]
35	$NO + O \rightarrow NO_2$	$\alpha_{NO2} = 2.6 \times 10^{-12}\,cm^3/molecules/s$	[35]
36	$NO + HO_2 \rightarrow OH + NO_2$	$\alpha_{O2N} = 8.85 \times 10^{-12}\,cm^3/molecules/s$	[21]
37	$NO_2 + H \rightarrow OH + NO$	$\alpha_{HO} = 1.47 \times 10^{-10}\,cm^3/molecules/s$	[36]
38	$NO_2 + OH \rightarrow HNO_3$	$\alpha_{HNO3} = 8.81 \times 10^{-11}\,cm^3/s$	[37]
39	$NO_2 + O \rightarrow O_2 + NO$	$\alpha_{O2} = 1.03 \times 10^{-11}\,cm^3/molecules/s$	[21]
40	$HO_2 + NO_2 \rightarrow HO_2NO_2$	$\alpha_{HONO} = 4.58 \times 10^{-12}\,cm^3/molecules/s$	[23]
41	$HNO_3 + OH \rightarrow H_2O + NO_3$	$\alpha_{NO3} = 1.5 \times 10^{-13}\,cm^3/s$	[35]

Table 1. Chemical reactions used for theoretical approaches in this study.

Results

Theoretical Approaches - Chemical species generated in plume of N_2 plasma jet with O_2. Various chemical species are generated from the N_2 plasma jet by changing the O_2 content in the plasma. The most predominant chemical species in the plasma jet is a metastable state N_2* [$N_2(A_3\sum_u^+)$] of excited nitrogen molecules. The rate coefficient α_{N2*} is expressed as[16]:

$$\alpha_{N2*}(T_e) = 2.25 \times 10^{-10}\sqrt{T_e}(6.8 + 2T_e)\exp\left(-\frac{6.8}{T_e}\right) \quad (1)$$

where, T_e is the electron temperature in a unit of eV. Dissociation coefficient of N_2 by electrons is given by:

$$k_N(T_e) = 4.26 \times 10^{-10}\sqrt{T_e}(10 + 2T_e)\exp(-10/T_e) \quad (2)$$

Meanwhile, the dissociation coefficient of $O_2$by electrons is given by[17]:

$$k_O(T_e) = 4.2 \times 10^{-9} \exp(-5.6/T_e) \quad (3)$$

The rate coefficients in Eqs (1–3) increase drastically as the electron temperature T_e increases. The reaction coefficients in Eqs (1–3) are given by $\alpha_{N2^*} = 6.40 \times 10^{-12}$, $k_N = 1 \times 10^{-12}$, and $k_O = 1.5 \times 10^{-11}$ cm^3/s for $T_e = 1$ eV, a typical value of non-thermal plasma.

The excited nitrogen molecules N_2* return back to the ground state when contact with N_2, according to $N_2(A_3\sum_u^+) + N_2 \rightarrow N_2 + N_2$ with its reaction coefficient of $\alpha_{N2} = 3 \times 10^{-18}$ cm^3/molecule/s[18]. The N_2* returns back to the ground state in contact with O_2 according to $N_2(A_3\sum_u^+) + O_2 \rightarrow$ products with its reaction coefficient of $\alpha_{O2} = 2.5 \times 10^{-12}$ cm^3/molecule/s[18]. The N_2* disappears in contact with water molecules[11] with a dissociation coefficient of $\alpha_{OH} = 5 \times 10^{-14}$ cm^3/s[18]. In these reactions, gas composition in jet is very important. If the ambient neutral density in the atmospheric pressure at room temperature is n_0, the N_2 and O_2 density in the entering gas can be expressed with oxygen mole fraction ξ. The O_2 density n_{O2} is ξn_0 and the N_2 density n_{N2} is $(1-\xi)n_0$. When the water molecules from the water surface are entering into this mixed gas with its mole fraction of ζ, the H_2O density n_{H2O} is ζn_0. The rate equation of the metastable state density n_{N2^*} can be calculated from

$$\frac{dn_{N2^*}}{dt} = \alpha_{N2^*}(1-\xi)(1-\zeta)n_0 n_p - [\alpha_{N2^*}(1-\xi) + \alpha_{O2}\xi + \alpha_{OH}\zeta]n_0 n_{N2^*} \quad (4)$$

where n_p is plasma electron density. The saturation time constant τ_{N2^*} of the metastable state molecules is $\tau_{N2^*} = [\alpha_{N2}(1-\xi)n_0 + \alpha_{O2}\xi n_0 + \alpha_{OH}\zeta n_0]^{-1} = [78(1-\xi) + 6.5 \times 10^7\xi + 1.3 \times 10^4\zeta]^{-1}$, which is less than the value of 100 μs for $n_0 = 2.6 \times 10^{19}$/cm^3 (the neutral density at ambient temperature in one atmospheric pressure) and $\xi = 0.001$ in a typical N_2 jet. N_2 gas at a flow rate of a liter per minute (lpm) is the working gas for the plasma jet, which length is up to a centimeter when the outlet diameter is 1 mm. Since the volume of the plume is about 10^{-2} liter, the fluid element may be in the plasma column for more than 600 μs. Hence, metastable state density may be approximated by the steady state value of $n_{N2^*} = \alpha_{N2^*}n_p/[\alpha_{N2}(1-\xi) + \alpha_{O2}\xi + \alpha_{OH}\zeta]$, which is estimated to be:

$$n_{N2^*} = 2.56(1-\xi)(1-\zeta)\eta \times 10^{12}/(\xi + 0.02\zeta + 0.0001) \quad (5)$$

particles/cm^3 for $T_e = 1$ eV, where the symbol η is the normalized plasma density defined by $\eta = n_p/10^{12}$. The N_2* are the beginning of most of the chemical reactions, being proportional to the plasma density. Therefore the overall trends of chemical reactions may not be very sensitive to the plasma density. Remember that the lifetime of N_2* in a metastable state is longer than 10 ms.

Penetration mechanism of N_2* in a metastable state into water. We investigate the penetration properties of N_2* entering into water, when a nitrogen plasma jet injects to a water surface. The N_2* in the plasma jet may continuously bombard on the water surface, diffuse into water, and generate hydroxyl molecules through a reaction with water molecules[11] with a dissociation coefficient of $\alpha_{OH} = 5 \times 10^{-14}$ cm^3/s[18]. Then, the diffusion equation of the N_2* in steady-state is given by $\nabla\Gamma_{N2^*} = \frac{dn_{N2^*}}{dt} = \alpha_{OH}n_{H2O}n_{N2^*}$[11]. Here, n_{H20} is the water density, and Γ_{N2^*} is the flux of N_2* defined by $\Gamma_{N2^*} = D\nabla n_{N2^*}$. The symbol D is the diffusion constant of the N_2*.

The diffusion constant D is calculated to be $D = 6.84 \times 10^{19}/n_{NT}$ in units of cm^2/s[11]. Introducing $\kappa_{N_2}^2 = \frac{\nabla^2 n_{N2^*}}{n_{N2^*}} = \alpha_{OH}n_{H2O}/D$, the diffusion equation for N_2* in water can be expressed as:

$$\frac{d^2 n_{N2^*}(z)}{dz^2} = \kappa_{N_2}^2 n_{N2^*}(z) \quad (6)$$

The solution to Eq. (6) is $n_{N2^*}(z) = n_{N0}\exp(-\kappa_{N_2}z)$. The density decay length λ_N is calculated to be 15 nm. This means that all N_2* will be instantaneously converted to hydroxyl and hydrogen atoms.

Generation of H, OH, HO_2 and H_2O_2 molecules in water. The OH and H molecules that were formed from the disappearance of N_2* at the water surface make consequence reactions to generate H, OH, HO_2, and H_2O_2. There are many ways to eliminate the H atoms, including $OH + H + M \rightarrow H_2O + M$ with its rate coefficient of $\alpha_{H2O} = 4.38 \times 10^{-30}(T_r/T)^2$ cm^6/mole^2/s $= 1.14 \times 10^{-10}$ cm^3/mole/s in air at $T = 300$ K[19], and $H + O_2 + M \rightarrow HO_2 + M$ with its reaction coefficient of: $\alpha_{O2H} = 1.78 \times 10^{-32}(T_r/T)^{0.8}$ cm^6/mole^2/s $= 4.6 \times 10^{-13}$ cm^3/s at $T = 300$ K[19], or $\alpha_{O2H} = 5.71 \times 10^{-32}(T_r/T)^{1.6}$ cm^6/mole^2/s $= 1.06 \times 10^{-12}$ cm^3/s at $T = 300$ K[20]. Here M is the neutral particles. There is a considerable difference of α_{O2H} in the references. However, we use α_{O2H} in ref.[19] in the subsequent analysis. Some of the H atoms generated from the N_2* may diffuse into water, and some of them may diffuse into gas. But most of them may disappear, forming H_2O and H_2O_2 molecules, due to the very high concentration of OH molecules in the water surface. Therefore, in the steady-state case, the H density can be calculated to be:

$$\begin{aligned} \alpha_{OH}n_{N2^*}n_{H2O} - \alpha_{H2O}n_{OH}n_H - \alpha_{O2H}n_{O2}n_H &= 0 \\ n_H = \alpha_{OH}n_{N2^*}n_{H2O}/((\alpha_{O2H} + \alpha_{H2O}x_{OH})n_0) & \end{aligned} \quad (7)$$

where, the symbol x_{OH} is the ratio of OH density to the ambient air density n_0.

There are many ways of disappearance of hydroxyl molecules. The dominant reactions of OH eliminations are forming H_2O_2 with its rate coefficient of $\alpha_{H2O2} = 6.83 \times 10^{-31}(T_r/T)^{0.8}$ cm^6/mole^2/s $= 1.78 \times 10^{-11}$ cm^3/mole/s in air at $T = 300$ K[21], and combining with HO_2 with its reaction coefficient of $\alpha_{OH2} = 4.8 \times 10^{-11}\exp(249/T) = 1.1 \times 10^{-10}$ cm^3/s[21]. Therefore, in the steady-state case, we obtain:

$$\alpha_{OH} n_{N2^*} n_{H2O} - \alpha_{H2O2} n_{OH} n_{OH} - \alpha_{H2O} n_{OH} n_{HO2} = 0 \quad (8)$$

The major sources of HO_2 radical composition are $H + O_2 + M \rightarrow HO_2 + M$ with its reaction coefficient of $\alpha_{O2H} = 4.6 \times 10^{-13}\,cm^3/s$[19], and combination of OH and H_2O_2 with its reaction coefficient of $\alpha_{HO2} = 1.7 \times 10^{-12}\,cm^3/s$[21]. The decay of HO_2 can be represented by $OH + HO_2 \rightarrow H_2O + O_2$, with its reaction coefficient of $\alpha_{OH2} = 4.8 \times 10^{-11} \exp(249/T) = 1.1 \times 10^{-10}\,cm^3/s$[21], which is one of the major destruction mechanism of OH radical. The density of n_{HO2} radical in steady state can be obtained from:

$$\alpha_{O2H} n_H \xi n_0 + \alpha_{HO2} n_{OH} n_{H2O2} - \alpha_{H2O} n_{OH} n_{HO2} = 0 \quad (9)$$

The hydrogen peroxide (H_2O_2) molecules are generated from the hydroxyl combination of $OH + OH + M \rightarrow H_2O_2 + M$, and are eliminated by reaction of $OH + H_2O_2 \rightarrow HO_2 + H_2O$, which are balanced by $\alpha_{H2O2} n_{OH}^2 = \alpha_{HO2} n_{OH} n_{H2O2}$, so the normalized H_2O_2 density can be obtained as:

$$x_{H2O2} = n_{H2O2}/n_0 = (\alpha_{H2O2}/\alpha_{HO2}) x_{OH} = 10 x_{OH}. \quad (10)$$

And the Eq. (9) is rewritten as to make the normalized HO_2 density as:

$$\alpha_{O2H} n_H \xi n_0 + \alpha_{H2O2} n_{OH}^2 - \alpha_{H2O} n_{OH} n_{HO2} = 0 \quad (11)$$

$$x_{HO2} = (\alpha_{H2O2}/\alpha_{H2O})(x_{OH} + \alpha_{O2H} x_H \xi/\alpha_{H2O2} x_{OH}) = 0.16(x_{OH} + 0.026 x_H \xi/x_{OH}). \quad (12)$$

However, when the hydroxyl density is very small, H_2O_2 may be generated from the reaction of $HO_2 + HO_2 \rightarrow H_2O_2 + O_2$ with its reaction coefficient of $\alpha_{H2O2} = 1.24 \times 10^{-12}\,cm^3/molecules/s$[22], and disappeared by the reaction of $H_2O_2 + O \rightarrow HO_2 + OH$ with its reaction of $\alpha_{O2H} = 1.7 \times 10^{-15}\,cm^3/molecules/s$[21], by $HO_2 + H_2O_2 \rightarrow OH + H_2O + O_2$ with its reaction coefficient of $1 \times 10^{-13}\,cm^3/molecules/s$[23], and by the reaction of $H_2O_2 + H \rightarrow OH + H_2O$ with its reaction coefficient of $4.2 \times 10^{-14}\,cm^3/molecules/s$[19]. Then normalized H_2O_2 density can be obtained as $x_{H2O2} = n_{H2O2}/n_0 = \left[(\alpha_{H2O2}/\alpha_{HO2}) x_{OH} + (\alpha_{H2O2}/\alpha_{HO2}) x_{HO2^2}^2/x_{OH}\right]/(1 + 0.001 x_O/x_{OH}) = [10 x_{OH} + 0.729 x_{HO2^2}/x_{OH}]/(1 + 0.001 x_O/x_{OH} + 0.588 x_{HO2}/x_{OH} + 0.0247 x_H/x_{OH})$.

Making use of Eqs (5, 7, 8 and 11), we obtain the normalized OH density equation as:

$$x_{OH}^2 + 2bx_{OH} - c = 0 \quad (13)$$

where, the constants b and c are defined by:

$$b = 4.7 \times 10^{-3} \xi\,;\; c = 1.76 \times 10^{-8} \frac{(1-\xi)(1-\zeta)\eta}{\xi + 0.02\zeta} \quad (14)$$

The meaningful solution of Eq. (13) is $x_{OH} = n_{OH}/n_0 = \sqrt{b^2 + c} - b$.

Hydrogen atoms are generated through a reaction between the excited nitrogen and water molecules[18], and $N + OH \rightarrow NO + H$[24], but the reaction between the excited nitrogen and water molecules prevails, due to the high concentration of water. The major elimination of H atoms is $H + O_2 + M \rightarrow HO_2 + M$ with its reaction coefficient of $\alpha_{O2H} = 5.71 \times 10^{-32} (T_r/T)^{1.6}\,cm^6/mole^2/s = 1.06 \times 10^{-12}\,cm^3/s$ at $T = 300\,K$[20], and forming water by hydrogen atom and hydroxyl[11] with a reaction coefficient of $\alpha_{H2O} = 1.1 \times 10^{-10}\,cm^3/s$[19], establishing the hydrogen atom density of $n_H = \alpha_{OH} n_{N2} n_{H2O}/(\alpha_{O2H} n_{O2} + \alpha_{H2O} n_{OH})$, which can be further simplified to:

$$x_H = \frac{n_H}{n_0} = 5.89 \frac{(1-\xi)(1-\zeta)}{(\xi + 108 x_{OH})(\xi + 0.02\zeta)} \times 10^{-6} \quad (15)$$

being the normalized H atom density.

Figure 1 shows plots of the normalized density of OH, H, and HO_2 molecules, x_{OH}, x_H, x_{O2H}, which are normalized by the neutral density at ambient air $n_0 = 2.6 \times 10^{19}/cm^3$. We assume the water density near the water surface is $\zeta = 0.60$ (60%), where most of the OH molecules are generated and diffused into water. On the other hand, the H atoms participating in chemical reactions with O and N atoms are borne far away from the water surface, where the water density is about $\zeta = 0.25$. The OH molecular density and H atom density decrease as the O_2 mole fraction ξ increases from zero to 0.25. On the other hand, the HO_2 density increases drastically as the ξ increases to 0.25.

Generation of reactive NH, NH_2, and NH_3 molecules in water. For generation of reactive nitrogen species (RNS), the generation of N atom is necessary. Electrons in the N_2 plasma generate N atoms by impact dissociation of N_2. The N atoms in the plasma jet may disappear according to the reaction of $N + O_2 \rightarrow NO + O$ with its reaction coefficient of $\alpha_{NO} = 9.22 \times 10^{-17}\,cm^3/mole/s$[22], to the reaction of $N + O \rightarrow NO$ with its reaction coefficient of $\alpha_{NO} = 2.39 \times 10^{-13}\,cm^3/mole/s$[25], to the reaction between hydroxyl and nitrogen atom with its reaction coefficient of $\alpha_{NO} = 4.7 \times 10^{-11}\,cm^3/molecules/s$[19], and to the reaction between hydrogen and nitrogen atoms with a reaction coefficient of $\alpha_{NH} = 1.3 \times 10^{-12}\,cm^3/s$[26]. But most of the OH molecules and H atoms are generated near the water surface. On the other hand, the N atoms are generated at the beginning of plasma jet far away from the water surface. Therefore, the OH molecules and H atoms may not actively participate in the disappearance process of N atoms. Thus the rate equation of the nitrogen atom density n_N is calculated from

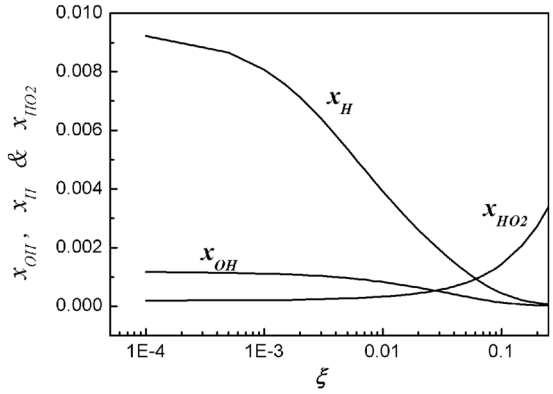

Figure 1. Plots of normalized density of hydroxyl molecule (x_{OH}), hydrogen atom (x_H), and hydrogen dioxide (x_{HO2}) versus the oxygen molecular mole fraction ξ. The analytical results in Fig. 1 show that as the oxygen mole fraction ξ increases from zero to 25%, the hydroxyl molecular density and hydrogen atom density decrease. On the other hand, as the oxygen mole fraction ξ increases to $\xi = 0.25$, the hydrogen dioxide density (x_{HO2}) drastically increases.

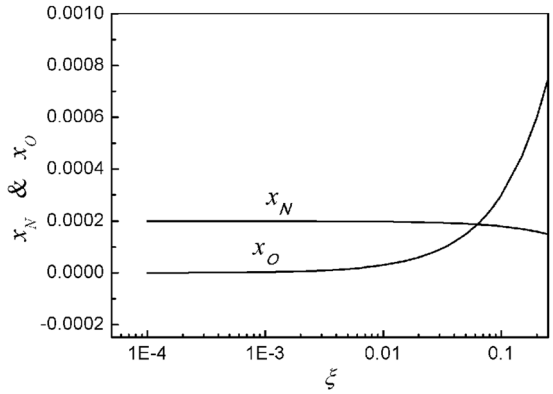

Figure 2. Plots of normalized nitrogen (x_N) and oxygen (x_O) atoms densities versus oxygen molecular mole fraction of ξ. As the oxygen molecular mole fraction of ξ increases, the oxygen atom density x_O increases drastically. However, in the entire range of the oxygen mole fraction, the nitrogen atom density is almost constant.

$$\frac{dn_N}{dt} = 2k_N(1-\xi)(1-\zeta)n_0 n_p - (\alpha_{O2N}\xi n_0 + \alpha_{NO}n_O)n_N$$

where, the N atom density may not saturate in the plasma column, because of insufficient O_2 mole fraction. The rate equation of oxygen atom density n_O is given by:

$$\frac{dn_O}{dt} = 2k_O\xi n_0 n_p - \alpha_{NO}n_O n_N$$

where, the O atom density also may not saturate in the plasma jet, continuously growing with time. Assuming the electron temperature of $T_e = 1$ eV, we find from the above two equations that the N and O atom normalized densities are $x_N = 2\times10^{-4}(1-\xi)(1-\varsigma)\eta/\mathrm{cm}^3$ and $x_O = 3\times10^{-3}(1-\varsigma)\eta\xi/\mathrm{cm}^3$ at $t = 100\,\mu$s, respectively.

Figure 2 shows plots of the normalized N and O atom densities in terms of the O_2 mole fraction of ξ. The O atom density x_O increases drastically as ξ increases. Here, these atom densities are determined at the time $t = 100$ μs, when the plasma jet injects into the water with a limited size of jet length, which is less than 1 cm. The O and N atoms are generated from the beginning very near the jet exit. Hydrogen atoms already start the chemical reactions from this jet exit.

The NH generation process is forming NH by combination of nitrogen and hydrogen atoms, while the major contributions to NH dissociation are the reaction between NH and hydroxyl forming HNO with a reaction coefficient of $\alpha_{HNO} = 3.32\times10^{-11}\,\mathrm{cm}^3/\mathrm{s}$[27], the reaction between NH and oxygen atom with the reaction coefficient of $\alpha_{OH} = 1.16\times10^{-11}\,\mathrm{cm}^3/\mathrm{molecules/s}$[28], and the reaction of $NH + O_2 \rightarrow$ Products with its reaction coefficient of $\alpha_{\mathrm{Pro}} = 9.98\times10^{-15}\,\mathrm{cm}^3/\mathrm{molecules/s}$[26], establishing the steady-state value of $n_{NH} = (\alpha_{NH}/\alpha_{HNO})(n_H n_N/[n_{OH} + \alpha_{OH}n_O/\alpha_{HNO} + \alpha_{pro}n_{O2}/\alpha_{HNO}])$ rather quickly; therefore, the normalized NH density is expressed

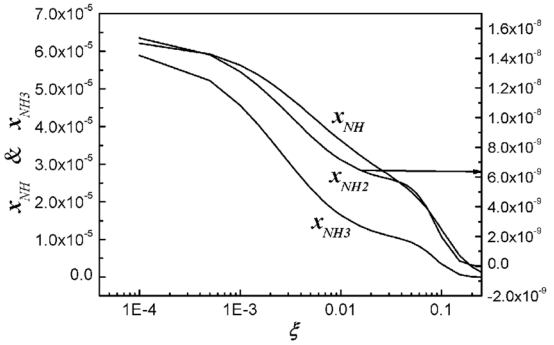

Figure 3. Plots of normalized densities of NH, NH_2, and NH_3 molecules versus the oxygen mole fraction of ξ. NH, NH_2, and Ammonia (NH_3) are well generated in the nitrogen plasma, due to the abundance of hydrogen atoms. However, as the oxygen mole fraction increases, they disappear very quickly. Nevertheless, ammonia generated in the nitrogen plasma jet dissolves into water forming ammonia water, which is a weak alkali.

as $x_{NH} = 3.9 \times 10^{-2} x_H\, x_N/[x_{OH} + 0.35x_O + 0.0003\xi(1-\varsigma)\eta]$, which is usually less than the N atom density. Combination of two NH molecules form NH_2[11] with a reaction coefficient of $\alpha_{NH2} = 4.3 \times 10^{-13}\,cm^3/s$[29], and NH_2 molecules are eliminated by reaction between NH_2 and OH forms NH_2OH with a reaction coefficient of $\alpha_{NH2OH} = 9.31 \times 10^{-11}\,cm^3/s$[30], by the reaction of NH_2 and O forming HNO with its reaction coefficient of $\alpha_H = 7.47 \times 10^{-11}\,cm^3$/molecules/s, and by the reaction of $O_2 + NH_2 \rightarrow H_2NOO$ with its reaction coefficient of $\alpha_{H2NOO} = 1.54 \times 10^{-15}\,cm^3$/molecules/s, leading to a steady-state value of $n_{NH2} = (\alpha_{NH2}/\alpha_{NH2OH})(n_{NH}{}^2/[n_{OH} + \alpha_H n_O/\alpha_{NH2OH} + \alpha_{H2NOO} n_{O2}])$, which can be expressed as $x_{NH2} = n_{NH2}/n_0 = 4.62 \times 10^{-3} x_{NH}{}^2/[x_{OH} + 0.8x_O + 1.65 \times 10^{-5}\xi(1-\varsigma)]$. The ammonia molecules are generated from the reaction of $H + NH_2 \rightarrow NH_3$ with its reaction coefficient of $\alpha_{NH3} = 7.7 \times 10^{-11}\,cm^3$/molecules/s[31], and the reaction between HNO_3 and NH_2 forming NH_3 with its reaction coefficient of $\alpha_{NH3} = 3.64 \times 10^{-13}\,cm^3$/molecules/s[32]. Meanwhile, the ammonia may be eliminated by the reaction of NH_3 and O with its reaction coefficient of $\alpha_{OH} = 4.69 \times 10^{-17}\,cm^3$/molecules/s[27], by the reaction between OH and NH_3[11] with its reaction coefficient of $\alpha_{H2O} = 1.6 \times 10^{-13}\,cm^3$/molecules/s[21], and by the reaction of NH_3 and NO_3 forming HNO_3 with its reaction coefficient of $\alpha_{HNO3} = 6 \times 10^{-16}\,cm^3$/molecules/s[33], leading to a steady-state value of the normalized ammonia density of $x_{NH3} = n_{NH3}/n_0 = 481(x_H + 0.0047 n_{HNO3})x_{NH2}/(x_{OH} + 0.000293x_O)$, where x_{HNO3} is the normalized density of nitric acid HNO_3.

Figure 3 shows plots of the normalized densities of NH, NH_2, and NH_3 molecules in terms of the oxygen mole fraction of ξ. Ammonia (NH_3) is well generated in the N_2 plasma, due to the abundance of H atoms. However, this compound disappears very quickly, as the O_2 mole fraction increase. Nevertheless, ammonia generated in the N_2 plasma jet dissolve into water, forming ammonia water, which is a weak alkali.

Generation of reactive NO, HNO_2, and HNO_3 molecules in water. We must investigate the nitric oxide behaviors in the environment of high concentration of H atoms in the vicinity of the water surface. Nitric monoxide is formed by the reaction of $N + OH \rightarrow NO + H$, by the reaction of $N + O \rightarrow NO$, and by the reaction of $N + O_2 \rightarrow NO + O$ with its reaction coefficient of $\alpha_{NO} = 9.22 \times 10^{-17}\,cm^3$/mole/s[22]; but its disappearance may be the reaction of NO and H forming HNO with its reaction coefficient of $\alpha_{HNO} = 1.56 \times 10^{-12}\,cm^3$/molecules/s[34], and the reaction of NO and OH forming HNO_2 with a reaction coefficient α_{HNO2} of $1.78 \times 10^{-11}\,cm^3/s$[22]. In this case, the nitrogen monoxide density is given by $n_{NO} = (\alpha_{NO}/\alpha_{HNO})(n_{OH} + n_O + \alpha_{NO2} n_{O2}/\alpha_{NO}) n_N/(n_H + \alpha_{HNO2} n_{OH}/\alpha_{HNO} + \alpha_{NO2} n_O/\alpha_{HNO})$, which can be expressed as $x_{NO} = 30.1(x_{OH} + 0.0051x_O + 0.000002\xi)x_N/(x_H + 11.4x_{OH} + 1.67x_O)$. The nitrous acid HNO_2 is destroyed due by the reaction of HNO_2 and OH with a reaction coefficient of $\alpha_{HNO2} = 5.95 \times 10^{-12}\,cm^3/s$[21], resulting to the steady-state value of the HNO_2 density of $n_{HNO2} = 3n_{NO}$. The leading reactions of NO_2 formation are the reaction of $NO + O \rightarrow NO_2$ with its reaction coefficient of $\alpha_{NO2} = 2.6 \times 10^{-12}\,cm^3$/molecules/s[35], the reaction between HNO_2 and OH forming NO_2[11], and the reaction of $NO + HO_2$ forming NO_2 with its reaction coefficient of $\alpha_{NO2} = 8.85 \times 10^{-12}\,cm^3$/molecules/s[21]. The leading elimination of NO_2 is the reaction of NO_2 and H with its reaction coefficient of $\alpha_{OH} = 1.47 \times 10^{-10}\,cm^3$/molecules/s[36], the reaction of NO_2 with OH forming HNO_3 with a reaction coefficient of $\alpha_{HNO3} = 8.81 \times 10^{-11}\,cm^3/s$[37], the reaction of $NO_2 + O \rightarrow O_2 + NO$ with its reaction coefficient of $\alpha_{O2} = 1.03 \times 10^{-11}\,cm^3$/molecules/s[21], and the reaction of $HO_2 + NO_2 \rightarrow HO_2NO_2$ with its reaction coefficient of $\alpha_{HONO} = 4.58 \times 10^{-12}\,cm^3$/molecules/s[23]. Therefore, the steady-state value of NO_2 density is given by $n_{NO2} = (\alpha_{HNO2}/\alpha_{OH})(3n_{OH} + 3n_{OH} + \alpha_{NO2} n_O/\alpha_{HNO2} + \alpha_{NO2} n_{HO2}/\alpha_{HNO2}) \times n_{NO}(n_H + \alpha_{HNO3} n_{OH}/\alpha_{OH} + \alpha_{O2} n_O/\alpha_{OH} + + \alpha_{HONO} n_{HO2}/\alpha_{OH})$, which is expressed as $x_{NO2} = 0.0405(3x_{OH} + 0.437x_O + 1.5x_{HO2})x_{NO}/(x_H + 0.6x_O + 0.07x_O + 0.0312x_{HO2})$. The nitric acid ($HNO_3$) can be eliminated by the reaction of HNO_3 with OH forming NO_3 with a reaction coefficient of $\alpha_{NO3} = 1.5 \times 10^{-13}\,cm^3/s$[35], leading to $x_{HNO3} = 587x_{NO2}$, and resulting in a very high concentration of nitric acid. We remind the reader that the H atom density n_H is very high for a small mole fraction of oxygen, so that in general, the nitric oxide densities for a small mole fraction of O_2 are very low. Therefore, the nitric acid density of n_{HNO3} is low for a small mole fraction of oxygen. On the other hand, the nitric acid density at a high mole fraction of O_2 is very high for a high value of nitric oxide density.

Figure 4 shows estimations of the nitric acid compounds in terms of the O_2 mole fraction. The nitric acid density (x_{HNO3}) is low at a small mole fraction of oxygen, but its intensity increases to a peak value of around $\xi \approx 0.2$, and then deceases, as the ξ increases. Meanwhile, the densities of HNO_2 and NO are at moderate levels in the

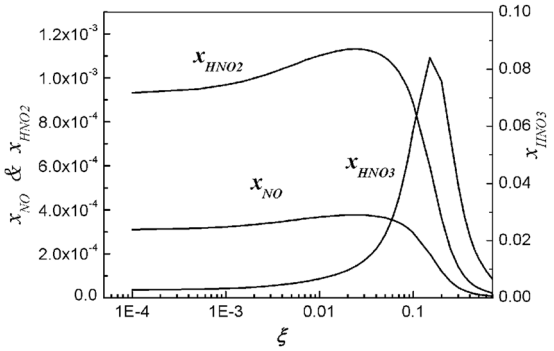

Figure 4. Plots of normalized densities of NO, HNO2, and HNO3 versus the oxygen mole fraction of ξ. At a small mole fraction of oxygen, the nitric acid density (x_{HNO3}) is low; but as the oxygen mole fraction increases, its intensity increases to a peak value of around $\xi \approx 0.2$, and then deceases. Meanwhile, in the range of $\xi \leq 0.25$, the densities of HNO_2 and NO are at a moderate level. The entire range of the oxygen mole fraction shows the existence of a moderate level of nitrogen monoxide (NO).

range of $\xi \leq 0.25$. Note that HNO_3 is a strong acid; meanwhile, HNO_2 is a weak acid. We remind the reader that a moderate level of nitrogen monoxide (NO) exists in the entire range of the O_2 mole fraction.

pH change in water activated by nitrogen plasma jet with oxygen. The ammonia can be dissolved into water forming NH_4OH, which turns the water alkali, increasing the *pH* value of the water. Meanwhile, the nitric acid HNO_3 also dissolves into water, making the water acidic with reducing *pH* value. Assuming the initial deionized water with its *pH* value of γ, the initial mole fractions of H^+ and OH^- ions are given by $[H^+] = 10^{-\gamma}$ and $[OH^-] = 10^{\gamma-14}$. Note that NH_4OH is a weak alkali, so that its electrolysis in water is partial. On the other hand, HNO_3 is a strong acid, so that its electrolysis in water is full. In this context, it is very difficult to analytically determine the *pH* value of water mixed with NH_4OH and HNO_3. However, we observed from Figs 3 and 4 that the ammonia (x_{NH3}) dominates over the nitric acid (x_{HNO3}) at a very small value of the O_2 mole fraction of $\xi \leq 10^{-4}$, being alkali. On the other hand, the intensity of nitric acid is strong for the O_2 mole fraction of $\xi \geq 0.01$, turning the plasma activated water to acidic.

Experimental Approaches

We compare the theoretical results with the experimentally measured data.

Figure 5 is a plot of the OH density in deionized water activated by the N_2 plasma jet. Most of the hydroxyl molecules are generated at water surface, and some of them can penetrate into water. We do not know what fraction of hydroxyl molecules are injected into the water. Therefore, the theoretical result obtained from $x_{OH} = n_{OH}/n_0 = \sqrt{b^2 + c} - b$ is least-squared-fitted to the experimental data, where the symbols b and c are expressed in Eq. (14) in terms of the O_2 mole fraction ξ. Typical error bar is shown in the data at $\xi = 0.003$, where the size of the error bar due to the experimental process is about 8% of its measurement value. Every experimental datum was determined by three times of measurements. Figure 5 clearly shows that the hydroxyl density is strong at a small ξ, but it quickly disappears as ξ increases to 0.2, corresponding to the O_2 mole fraction of air.

Figure 6 is the experimental data of the NH_4^+ ion concentration in water in terms of the O_2 mole fraction ξ. Based on a previous report[38], we assume that the ammonia of NH_3 may dissolve into water forming ammonia water, where NH_4^+ ions may be generated. The concentration of NH_4^+ ions plays an important role in determination of *pH* value in water. Therefore, the theoretical result (curve) of ammonia obtained from $x_{NH3} = n_{NH3}/n_0 = 48\,1(x_H + 0.0047 n_{HNO3})x_{NH2}/(x_{OH} + 0.000293 x_O)$ or from Fig. 3 will be least-squared-fitted to the experimental data of NH_4^+ concentration. The vertical axis in the right represents the ammonia concentration in the plasma jet in ppm unit. The typical error bar is shown in the data at $\xi = 0.01$, where the size of the error bar due to the experimental process is about 11% of its measurement value. The experimental data follows the trend of the theoretical results. The ammonia concentration decreases as ξ increases to 0.2.

Figure 7 is the experimental data of the NO_3^- ion concentration in water, in terms of the O_2 mole fraction of ξ. The theoretical results (curve) obtained from Fig. 4 in terms of HNO_3 are also plotted in this figure, reasonably assuming that the nitric acid of HNO_3 is dissolving into water. The theoretical results are least-squared-fitted to the experimental data. The typical error bar is shown in the data at $\xi = 0.05$, where the size of the error bar due to the experimental process is about 10% of its measurement value. It is obvious from Fig. 7 that the experimental data and theoretical result indicate the increase of nitric acid as ξ increases to 0.2. However, the theoretical curve in Fig. 4 indicates that as the ξ increases beyond 0.2, the nitric acid (HNO_3) deceases drastically.

One of the most important reactive chemicals in water is the H_2O_2 generated from N_2 plasma jet. Figure 8 shows a plot of the measurement data (dots) of the H_2O_2 in water activated by a N_2 plasma jet with changing O_2 mole fraction of ξ. The theoretical curve obtained from $x_{H2O2} = n_{H2O2}/n_{0=}[10x_{OH} + 0.729x_{HO2}^2/x_{OH}]/(1 + 0.001x_O/x_{OH} + 0.588x_{HO2}/x_{OH} + 0.0247x_H/x_{OH})$ is least-squared-fitted to the experimental data. The typical error bar is shown in the data at $\xi = 0.005$, where the size of the error bar due to the experimental process is about 9% of its measurement value. The intensity of the H_2O_2 is very high at a small value of ξ, where a relatively high intensity of hydroxyl generates H_2O_2, as expected from Fig. 1. But similar to the hydroxyl density, its intensity decreases

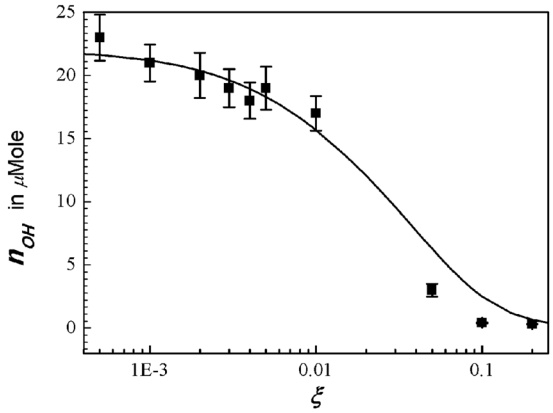

Figure 5. Plot of hydroxyl density in deionized water activated by the nitrogen plasma jet versus the oxygen mole fraction of ξ. Dots in the figure are the experimental data from the averaged value of three times of measurements. The hydroxyl molecules are mostly generated at water surface, and some of them can penetrate into water. The theoretical result (curve) obtained from $x_{OH} = n_{OH}/n_0 = \sqrt{b^2 + c} - b$ is least-squared-fitted to the experimental data, where the symbols b and c are expressed in Eq. (14) in terms of the oxygen mole fraction ξ. The typical error bar is shown in the data at the oxygen mole fraction $\xi = 0.003$, where the size of the error bar due to the experimental process is about 8% of its measurement value. At a small mole fraction of oxygen, the hydroxyl density is strong; but as the oxygen mole fraction increase to 0.2, corresponding to the oxygen mole fraction of air, it quickly disappears.

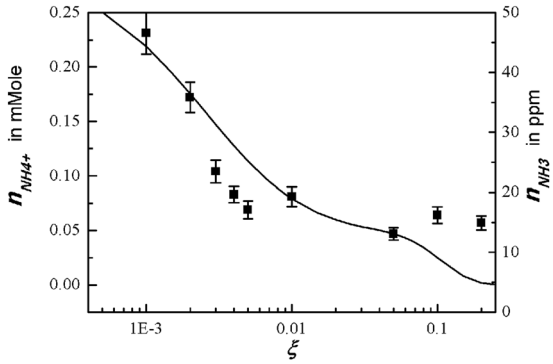

Figure 6. Plot of experimental data of NH_4^+ ion concentration in water versus oxygen mole fraction of ξ. The ammonia of NH_3 may dissolve into water forming ammonia water, where NH_4^+ ions may be generated. The theoretical result (curve) of ammonia obtained from $x_{NH3} = n_{NH3}/n_0 = 481(x_H + 0.0047 n_{HNO3})x_{NH2}/(x_{OH} + 0.000293 x_O)$ or from Fig. 3 is least-squared-fitted to the experimental data of NH_4^+ concentration. The typical error bar is shown in the data at the oxygen mole fraction $\xi = 0.01$, where the size of the error bar due to experimental process is about 11% of its measurement value. The experimental data follows the trend of the theoretical results. As the oxygen mole fraction increases to $\xi = 0.2$, the ammonia concentration decreases.

as ξ increases. However, the H_2O_2 density increases again as ξ increases to a large value. The rebounding increase of H_2O_2 at a large value of ξ is caused by a strong surge of HO_2 molecules shown in Fig. 1, which generate H_2O_2 molecules. Therefore, the density of H_2O_2 deceases, reaches its minimum value at $\xi = 0.05$, and then increases again, as the ξ increases from a small value to a large value. The experimental data follow the theoretical trend, but there are some deviations from the theoretical curve. Further study is needed to resolve this difference in future.

Finally, we like to investigate the *pH* of water activated by the nitrogen plasma by changing the oxygen mole fraction of ξ. Figure 9 is the experimental data of the *pH* values of water activated by the nitrogen plasma. The *pH* value was measured in terms of the oxygen mole fraction. The typical error bar is shown in the data at the oxygen mole fraction $\xi = 0.01$, where the size of the error bar due to measurement process is about 10% of its measurement value. As expected in the analytical study, the plasma activated water is alkali at a very small value of the oxygen mole fraction, due to the high density of ammonia, and then it becomes acidic as the oxygen mole fraction increases to a large value. The *pH* of the plasma activated water at $\xi = 0.2$ corresponding to air is about 3.

Discussion

The purpose of this study is the investigation of the influence of O_2 on the generation of reactive chemical species from a N_2 plasma jet near a water surface. The most abundant reactive species in a N_2 plasma jet is the excited

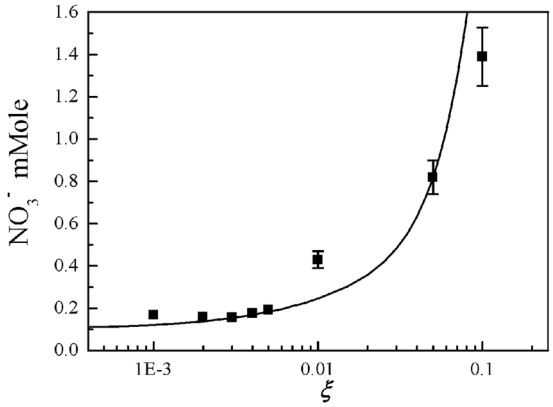

Figure 7. Plots of the experimental data of NO_3^- ion concentration in water versus oxygen mole fraction of ξ. The theoretical results in Fig. 4 are least-squared-fitted to the experimental data. The typical error bar is shown in the data at the oxygen mole fraction $\xi = 0.05$, where the size of the error bar due to the experimental process is about 10% of its measurement value. As the oxygen mole fraction of ξ increases to $\xi = 0.2$, the experimental data and theoretical result (curve) indicate the increase of nitric acid. However, the theoretical curve in Fig. 4 indicates that as the oxygen mole fraction increases beyond $\xi = 0.2$, the nitric acid (HNO_3) deceases drastically.

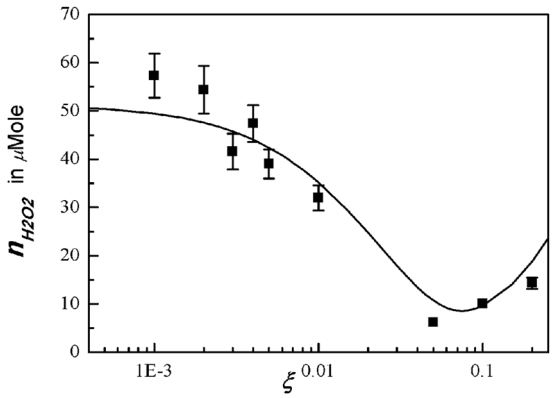

Figure 8. Plot of experimental data (dots) of the hydrogen peroxide versus the oxygen mole fraction ξ. At a small value of oxygen mole fraction, the intensity of the hydrogen peroxide is very high, where a relatively high intensity of hydroxyl generates H_2O_2, as expected from Fig. 1. But as the oxygen mole fraction increases, its intensity decreases, like the hydroxyl density. However, as the oxygen mole fraction increases to a large value, the hydrogen peroxide density increases again, due to the strong surge of hydrogen dioxide molecules shown in Fig. 1. Therefore, as the oxygen mole fraction increases from a small value to a large value, the hydrogen peroxide density deceases, reaches its minimum value at $\xi = 0.05$, and then increases again.

nitrogen molecules in the metastable state of N_2*, which in turn dissociate water molecules, generating hydroxyl (OH) molecules and hydrogen atoms near the water surface. A presence of oxygen molecules may obstruct the dissociation mechanism of water molecules by the excited nitrogen molecules. In this regard, we theoretically and experimentally investigate the reactive chemical species in nitrogen plasma by changing the O_2 mole fraction of ξ.

Various chemical compounds are fabricated from N_2* and water molecules in plasma jet with varying O_2 content. Detailed theoretical investigation of these chemical compounds is carried out in terms of different O_2 content. Hydroxyl molecules and hydrogen atoms are well fabricated near the water surface by a nitrogen plasma jet without oxygen. But Fig. 1 shows that the densities of those species decrease as ξ increases. On the other hand, the density of the hydrogen dioxide increases drastically as ξ increases, turning the hydroxyl molecules into water. Due to the high density of hydrogen atoms, the ammonia intensity is relatively high at a small value of ξ. But Fig. 3 shows that the ammonia density (x_{NH3}) decreases drastically as ξ increases. Nitrogen monoxide (NO) is one of the important molecules related to a signaling material in cells. Figure 4 shows that the density of nitrogen monoxide is at a moderate level over the entire range $\xi \leq 0.2$. Nitric acid (HNO_3) starts from a negligibly small value, increases to a peak value at $\xi \approx 0.2$, and then decreases, as ξ increases to a large value.

Electrons in plasma jet may have active roles in electron-impact ionization, excitation, dissociations, etc. There are hundreds chemical reactions of N, H, O elements in "plasma and humid air" or "plasma at water boundary" with electrons involved. Some of these reactions may play important roles. Investigating all of these reactions may be beyond the scope of this article. We therefore consider the most important reactions associated with negative affinity of oxygen. As a first example, water molecules made of oxygen may undergo a dissociative

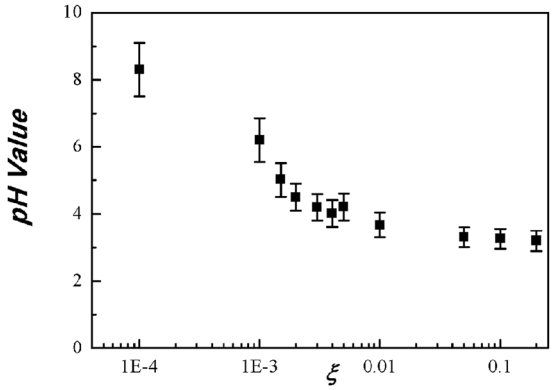

Figure 9. Plots of experimental data of the *pH* values of water activated by the nitrogen plasma versus the oxygen mole fraction of ξ. The typical error bar in this experiment is shown in the data at the oxygen mole fraction $\xi = 0.01$, where the size of the error bar due to measurement process is about 10% of its measurement value. As expected in the analytical study, at a very small value of the oxygen mole fraction, the plasma activated water is alkali, and as the oxygen mole fraction increases to a large value, it becomes acidic The *pH* of the plasma activated water at $\xi = 0.2$ corresponding to air is about 3.

attachment by the reaction of $e + H_2O \rightarrow H^- + OH$ with the dissociative-attachment coefficient of α_{da}. This reaction is important because of hydroxyl production. However, the excitation cross section of nitrogen molecules is one order in magnitude larger than the dissociative-attachment cross section of water, thereby estimating to be $\alpha_{N2*} = 6.4 \times 10^{-12}\,cm^3/s$ and $\alpha_{da} = 9 \times 10^{-13}\,cm^3/s$ at $T_e = 1\,eV$[17,39]. The dominant gas in the plasma jet is nitrogen molecules so that the density of the metastable state N_2* is $2.6 \times 10^{16}/cm^3$ due to a long lifetime[11], dissociating water molecules by reaction of $N_2(A_3\sum_u{}^+)$ and H_2O with a dissociation coefficient[19] of $\alpha_{OH} = 5 \times 10^{-14}\,cm^3/s$. On the other hand, the electron density may be considerably less than $10^{12}/cm^3$ as approaching water surface due to various reasons including spreading, recombination, electron attachment, diffusions, etc. The product of $(2.6 \times 10^{16}/cm^3)$ $(5 \times 10^{-14}\,cm^3/s)$ is $1.3 \times 10^3/s$, whereas the product of $(10^{12}/cm^3)$ $(9 \times 10^{-13}\,cm^3/s)$ is $9 \times 10^{-1}/s$. Therefore, the dissociative attachment of water molecules by electrons may be negligible in comparison with water dissociation by $N_2(A_3\sum_u{}^+)$. The other important reaction of the electron affinity is the dissociative attachment of oxygen molecules by $e + O_2 \rightarrow O^- + O$ with dissociative attachment coefficient of k_{da}, which is less than one fifth of k_O in Eq. (3) at $T_e = 1\,eV$[40].

Experimental measurements of the reactive chemical species in the plasma activated water were also carried out by comparison with the theoretical results. This identified that hydroxyl molecules are mostly generated at water surface, and some of them can penetrate into water. The hydroxyl molecular density reaches its maximum without oxygen, and decreases to zero, as ξ increases to 0.25, showing that the theoretical prediction agrees reasonably well with the experimental data. The theoretical results and experimental data also indicate that the density of the ammonia of NH_3 also deceases as ξ increases to 0.25. On the other hand, theory and experiment show that the density of the NO_3 increases drastically as ξ increases to 0.25. The density of hydrogen peroxide in plasma activated water was measured. The hydrogen peroxide density deceases, reaches its minimum value at $\xi = 0.05$, and then increases again, as ξ increases from a small value to a large value. Although the experimental data of the hydrogen peroxide follow the theoretical trend, there are considerable deviations from the theoretical curve. Further study is therefore recommended in future to resolve this difference. The *pH* value of the water activated by the N_2 plasma jet is experimentally measured. The *pH* value of the plasma activated water, which is slightly alkali without oxygen, decreases to three as ξ increases to 0.25, which can be expected by the nitric acid in Fig. 4, and was also confirmed by experiments. The ξ of ambient air is about 0.2, so that the *pH* value of water activated by the air plasma is acidic, with $pH \approx 3$.

Method

Generation of the nitrogen plasma jet. A nonthermal plasma device is operated at atmospheric pressure inside a vacuum chamber filled with N_2 gas[41]. The plasma jet system is powered by a 60 Hz AC power supply using a neon transformer (PNP-1000, Daekwang Electric Co.). The inner electrode is a stainless-steel cylinder with an inner and outer diameters of 1.2 mm and 1.4 mm respectively, which is covered by a quartz tube with an outer diameter of 3.2 mm. The outer electrode is fabricated from stainless steel, and is centrally perforated with a hole of 1 mm, through which the plasma jet is ejected to the water surface in a dish surrounded by N_2 gas. The microdischarges in the porous alumina between inner and outer electrodes evolved into a plasma jet as the applied power increased. Significant changes in the discharge voltage and current waveforms were observed during the process of the evolution to the plasma jet. The current pulses were of short durations of 30–100 ns in the close-up image. They had repetition rates of 10–400 kHz and amplitudes reaching a few amperes and the discharge voltage of a few kV. This indicates that even at a frequency as low as 60 Hz, the plasma that evolves from a large amount of microdischarge inside a porous dielectric can have characteristics that are similar to those generated at several hundreds of kilohertz. The ratios of nitrogen and oxygen gases are controlled by a mass flow controller (GMC 1200, Atovac), and the total gas flow rate through the device is 1 liter per minute (lpm). In order to avoid the

influence of O_2 in the surrounding air, the experiment is carried out in a glove box, where the O_2 concentration is kept at less than 1%.

One of the most important issues in plasma jet is plasma properties represented by the electron temperature T_e and density n_p, which can vary very sensitively by oxygen mole fractionξ. The electron temperature increases as the oxygen mole fraction increases, whereas the electron density decreases instead[42,43]. The electron temperature T_e and density n_p may also be functions of measurement time and space in the plasma jet. We measured the electron temperature and density very close to the jet injection point near the electrodes. The electron temperature T_e is measured to be approximately 0.5 eV for $\xi = 0$ and 1.5 eV for $\xi = 0.2$, consistent to data in refs[42,43], whose experimental setups are very similar configuration to the present experiment. We therefore assume the electron temperature to be $T_e = 1$ eV in analytical calculation in our theoretical model. On the other hands, the plasma electron density varies in wide range according to the measurement point in the plasma jet, although the plasma density decreases drastically as the oxygen mole fraction increases, as expected. The electron density for $\xi = 0.2$ (air) is significantly less than that for $\xi = 0$ (nitrogen only) and is localized near electrodes even for higher discharge voltage due to electron attachment of oxygen molecules. The theoretical results in the analytical calculation based on the assumption of the electron density to be $n_p = 10^{12}/cm^3$ are least-squared-fitted to the experimental data in qualitative comparison, observing agreement between theoretical trend and experimental data. A study of plasma evolution in time and space for a given oxygen mole fraction is beyond the scope of present research and will be left for future work for customized investigation of individual experimental configurations.

Measurement of various chemical species and *pH* values in water. The deionized (DI) water is deoxygenized by N_2 purging before experiments, and 1 ml DI water is placed 5 mm below the electrode. DI water is treated with nonthermal plasma for 3 minutes, and the concentrations of OH·, H_2O_2, NO_2^-, NO_3^-, and NH_4^+, and the pH are measured. For OH· radical measurement, terephthalic acid (TA) that specifically reacts with OH· to become fluorescent hydroxyl-terephthalic (HTA) is used. Both TA (185361, Sigma-Aldrich Co) and HTA (752525, Aldrich) are solved in 35 mM NaOH solution to make 10 mM solutions, and the diluted HTA solution in TA solution is used as a standard to quantify OH· impinging on the TA solutions. The fluorescence intensity is measured using a spectrophotometer with a filter set of 340/420 nm (ex/em). For H_2O_2 measurement, Amplex UltraRed reagent (A36006, Invitrogen) is used following the manufacturer's protocol. NO_3^- and NH_4^+ ion concentrations are detected by ion chromatography method. The pH value is measured using a pH meter (pH Spear, Eutech Instruments). All liquid samples are treated by the APNP under the same conditions.

References

1. Kumar, N. *et al*. Enhancement of glucose uptake in skeletal muscle L6 cells and insulin secretion in pancreatic hamster-insulinoma-transfected cells by application of non-thermal plasma jet. *App. Phys. Lett.* **103**, 203701 (2013).
2. Fathollah, S. *et al*. Investigation on the effects of the atmospheric pressure plasma on wound healing in diabetic rats. *Sci Rep.* **6**, 19144, https://doi.org/10.1038/srep19144 (2016).
3. Vandamme, M. *et al*. ROS implication in a new antitumor strategy based on non-thermal plasma. *Int. J. Cancer.* **130**, 2185–2194 (2012).
4. Kaushik, N. *et al*. Non-thermal plasma with 2-deoxy-D-glucose synergistically induces cell death by targeting glycolysis in blood cancer cells. *Sci Rep.* **5**, 8726, https://doi.org/10.1038/srep08726 (2015).
5. Kumar, N. *et al*. Induced apoptosis in melanocytes cancer cell and oxidation in biomolecules through deuterium oxide generated from atmospheric pressure non-thermal plasma jet. *Sci Rep.* **4**, 7589, https://doi.org/10.1038/srep07589 (2014).
6. Panngom, K. *et al*. Preferential killing of human lung cancer cell lines with mitochondrial dysfunction by nonthermal dielectric barrier discharge plasma. *Cell. Death. Dis.* **4**, e642, https://doi.org/10.1038/cddis.2013.168 (2013).
7. Adachi, T. *et al*. Plasma-activated medium induces A549 cell injury via a spiral apoptotic cascade involving the mitochondrial–nuclear network. *Free Radical Bio. Med.* **79**, 28–44 (2015).
8. Wende, K. *et al*. Identification of the biologically active liquid chemistry induced by a nonthermal atmospheric pressure plasma jet. *Biointerphases.* **10**, 029518 (2015).
9. Lukes, P., Dolezalova, E., Sisrova, I. & Clupek, M. Aqueous-phase chemistry and bactericidal effects from an air discharge plasma in contact with water: evidence for the formation of peroxynitrite through a pseudo-second-order post-discharge reaction of H2O2 and HNO2. *Plasma Sources Sci. T.* **23**, 015019 (2014).
10. Van gils, C. A. J. *et al*. Mechanisms of bacterial inactivation in the liquid phase induced by a remote RF cold atmospheric pressure plasma jet. *J. Phy. D: Appl. Phys.* **46**, 175203 (2013).
11. Uhm, H. S. Generation of various radicals in nitrogen plasma and their behavior in media. *Phys. Plasmas.* **22**, 123506 (2015).
12. Takamatsu, T. *et al*. Investigation of reactive species using various gas plasmas. *RSC Adv.* **4**, 39901–39905 (2014).
13. Takamatsu, T. *et al*. Investigation of Reactive Species in Various Gas Plasmas Treated Liquid and Sterilization Effects. *Int. Society on Plasma Chem.* **21**, 370 (2013).
14. Burlica, R., Kirkpatrick, M. J. & Locke, B. R. Formation of reactive species in gliding arc discharges with liquid water. *J. Electrostat.* **64**, 35–43 (2006).
15. Baik, K. Y. *et al*. The Role of Free Radicals in Hemolytic Toxicity Induced by Atmospheric-Pressure Plasma Jet. *Oxid. Med. Cell. Longev.* **2017**, 1289041 (2017).
16. Uhm, H. S., Na, Y. H., Choi, E. H. & Cho, G. Dissociation and excitation coefficients of nitrogen molecules and nitrogen monoxide generation. *Phys. Plasmas.* **20**, 083502 (2013).
17. Liberman, M. A., Lichtenberg, A. J. Principal of Plasma Discharge and Material Processing. 225–227 (John Wiley and sons, 1994).
18. Herron, J. T. Evaluated chemical kinetics data for reactions of N(2D), N(2P), and N2(A3 Σu+) in the gas phase. *J. Phys. Chem. Ref. Data.* **28**, 1453–1483 (1999).
19. Baulch, D. L. *et al*. Evaluated kinetic data for combustion modeling. Supplement I. *J. Phys. Chem. Ref. Data.* **23**, 847–848 (1994).
20. Turányi, T. *et al*. Determination of rate parameters based on both direct and indirect measurements. *Int. J. Chem. Kinet.* **44**, 284–302 (2012).
21. Atkinson, R. *et al*. Evaluated kinetic and photochemical data for atmospheric chemistry: Volume I - gas phase reactions of Ox, HOx, NOx and SOx species. *Atmos. Chem. Phys.* **3**, 6179 (1997).
22. Demore, W. B. *et al*. Chemical Kinetics and Photochemical Data for Use in Stratospheric Modeling. Evaluation No 12. *JPL Publication.* **97**, 266 (1997).
23. Vardanyan, I. A., Sachyan, G. A., Philiposyan, A. G. & Nalbandyan, A. B. Kinetics and mechanism of formaldehyde oxidation—II. *Combustion Flame.* **22**, 153–159 (1974).

24. Atkinson, R. *et al*. Evaluated kinetic and photochemical data for atmospheric chemistry: Supplement III. IUPAC subcommittee on gas kinetic data evaluation for atmospheric chemistry. *J. Phys. Chem. Ref. Data.* **18**, 881 (1989).
25. Campbell, I. M. & Gray, C. N. Rate constants for O(3P) recombination and association with N(4S). *Chem. Phys. Lett.* **18**, 607–609 (1973).
26. Brown, R. L. A measurement of the rate of the reaction N + H + M → NH + M. *Int. J. Chem. Kinet.* **5**, 663 (1973).
27. Cohen, N. & Westberg, K. R. Chemical Kinetic Data Sheets for High-Temperature Reactions. Part II. *J. Phys. Chem. Ref. Data.* **20**, 1211–1311 (1991).
28. Tsang, W. & Hampson, R. F. Chemical kinetic data base for combustion chemistry. Part I. Methane and related compounds. *J. Phys. Chem. Ref. Data.* **15**, 1087–1279 (1986).
29. Xu, Z. F., Fang, D. C. & Fu, X. Y. Ab initio study on the reaction 2NH (X3Σ−) → NH2(X2B1) + N (4S). *Chem. Phys. Lett.* **275**, 386–391 (1997).
30. Fagerström, K., Jodkowski, J. T., Lund, A. & Ratajczak, E. Kinetics of the self-reaction and the reaction with OH of the amidogen radical. *Chem. Phys. Lett.* **236**, 103–110 (1995).
31. Schofield, K. Evaluated chemical kinetic rate constants for various gas phase reactions. *J. Phys. Chem. Ref. Data.* **2**, 25–84 (1973).
32. Xu, S. & Lin, M. C. Ab initio chemical kinetics for the NH2 + HNOx reactions, part III: Kinetics and mechanism for NH2 + HONO2. *Int. J. Chem. Kinet.* **42**, 69–78 (2010).
33. Cantrell, C. A. *et al*. Reactions of nitrate radical and nitrogen oxide (N2O5) with molecular species of possible atmospheric interest. *J. Phys. Chem.* **91**, 6017–6021 (1987).
34. Tsang, W. & Herron, J. T. Chemical kinetic data base for propellant combustion I. Reactions involving NO, NO2, HNO, HNO2, HCN and N2O. *J. Phys. Chem. Ref. Data.* **20**, 609–663 (1991).
35. Atkinson, R. *et al*. Evaluated kinetic and photochemical data for atmospheric chemistry: Supplement VI. IUPAC subcommittee on gas kinetic data evaluation for atmospheric chemistry. *J. Phys. Chem. Ref. Data.* **26**, 1329–1499 (1997).
36. Su, M. C. Rate constants, 1100 ≤ T ≤ 2000 K, for H + NO2 → OH + NO using two shock tube techniques: Comparison of theory to experiment. *J. Phys. Chem. A.* **106**, 8261–8270 (2002).
37. Donahue, N. M. *et al*. High-pressure flow study of the reactions OH + NOx → HONOx: Errors in the falloff region. *J. Geophys. Res.* **102**, 6159–6168 (1997).
38. Hales, J. M. & Drewes Solubility of ammonia in water at low concentrations. *Atmos. Environ.* **13**, 1133–1147 (1979).
39. Compton, R. N. & Christophorou, L. G. Negative-ion formation in H2O and D2O. *Phys. Rev.* **154**, 110–116 (1967).
40. Lee, C., Graves, D. B., Lieberman, M. A. & Hess, D. W. Global model of plasma chemistry in a high density oxygen discharge. *J. Electrochem. Soc.* **141**, 1546–1555 (1994).
41. Lee, C. B. *et al*. Evidence of radicals created by plasma in bacteria in water. *App. Phys. Lets.* **105**, 073702 (2014).
42. Hong, Y. C. & Uhm, H. S. Microplasma jet at atmospheric pressure. *App. Phys. Lets.* **89**, 221504 (2006).
43. Hong, Y. C. & Uhm, H. S. Air plasma jet with hollow electrodes at atmospheric pressure. *Phys. Plasmas.* **14**, 053503 (2007).

Acknowledgements

This research was supported by Leading Foreign Research Institute Recruitment Program through the National Research Foundation of Korea (NRF) funded by the Korea government (MSIP) (NRF-2016K1A4A3914113), and funded by NRF (NRF-2016R1A1A1A05005431). This work was also partially supported by Korea Technology Information Promotion Agency (SME-C0566231).

Author Contributions

H.S.U. and S.H.K. wrote the manuscript, performed the study and interpreted the results. K.Y.B. and E.H.C. supervised the study and provided assistance with experiment. E.H.C. contributed the materials.

Additional Information

Competing Interests: The authors declare no competing interests.

Publisher's note: Springer Nature remains neutral with regard to jurisdictional claims in published maps and institutional affiliations.